Cancer Letters 565 (2023) 216237

Contents lists available at ScienceDirect

Cancer Letters

journal homepage: www.elsevier.com/locate/canlet

A novel EGFR inhibitor acts as potent tool for hypoxia-activated prodrug systems and exerts strong synergistic activity with VEGFR inhibition *in vitro* and *in vivo*

Monika Caban [a,f,1], Bettina Koblmueller [a,1], Diana Groza [a,f], Hemma H. Schueffl [a,f], Alessio Terenzi [b], Alexander Tolios [c,d], Thomas Mohr [a], Marlene Mathuber [e,f], Kushtrim Kryeziu [a], Carola Jaunecker [a], Christine Pirker [a], Bernhard K. Keppler [e,f], Walter Berger [a,f], Christian R. Kowol [e,f], Petra Heffeter [a,f,*]

[a] Center for Cancer Research and Comprehensive Cancer Center, Medical University of Vienna, Austria
[b] Department of Biological, Chemical and Pharmaceutical Sciences and Technologies, University of Palermo, Italy
[c] Department of Transfusion Medicine and Cellular Therapy, Institute of Vascular Biology, Medical University of Vienna, AT-1090, Vienna, Austria
[d] Institute of Vascular Biology and Thrombosis Research, Center for Physiology and Pharmacology, Medical University of Vienna, Austria
[e] Institute of Inorganic Chemistry, Faculty of Chemistry, University of Vienna, Austria
[f] Research Cluster "Translational Cancer Therapy Research", University of Vienna and Medical University of Vienna, Austria

ARTICLE INFO

Keywords:
EGFR
VEGFR
Hypoxia
Prodrug
Cancer therapy
Cobalt
Tyrosine kinase inhibitor

ABSTRACT

Small-molecule EGFR inhibitors have distinctly improved the overall survival especially in EGFR-mutated lung cancer. However, their use is often limited by severe adverse effects and rapid resistance development. To overcome these limitations, a hypoxia-activatable Co(III)-based prodrug (KP2334) was recently synthesized releasing the new EGFR inhibitor KP2187 in a highly tumor-specific manner only in hypoxic areas of the tumor. However, the chemical modifications in KP2187 necessary for cobalt chelation could potentially interfere with its EGFR-binding ability. Consequently, in this study, the biological activity and EGFR inhibition potential of KP2187 was compared to clinically approved EGFR inhibitors. In general, the activity as well as EGFR binding (shown in docking studies) was very similar to erlotinib and gefitinib (while other EGFR-inhibitory drugs behaved different) indicating no interference of the chelating moiety with the EGFR binding. Moreover, KP2187 significantly inhibited cancer cell proliferation as well as EGFR pathway activation *in vitro* and *in vivo*. Finally, KP2187 proved to be highly synergistic with VEGFR inhibitors such as sunitinib. This indicates that KP2187-releasing hypoxia-activated prodrug systems are promising candidates to overcome the clinically observed enhanced toxicity of EGFR-VEGFR inhibitor combination therapies.

1. Introduction

About 10–15% of all Caucasian and 50% of all Asian patients with advanced or metastatic lung cancer develop tumors harboring an activating mutation of the epidermal growth factor receptor (EGFR) [1]. In addition, constitutive activation of this oncogene has also been observed in a number of other tumor types such as glioblastoma, colon as well as head and neck cancer [2–5]. This led to the development of a plethora of EGFR-targeted therapeutics, in form of either antibodies or small-molecules. The first EGFR-inhibitory small molecule which was approved for treatment of advanced non-small cell lung cancer was gefitinib, followed by erlotinib, two drugs which both inhibit the kinase activity of the receptor by docking into its ATP-binding pocket [6]. Later on, afatinib, which irreversibly binds into the receptor molecule, was developed. However, rapid drug resistance (in about 50% of all cases due to the T790M point mutation) prompted development of next generation tyrosine kinase inhibitors (TKIs), such as osimertinib, to target even these mutated EGFR molecules [6–8]. In addition, there are several other multi-kinase inhibitors with EGFR-inhibiting properties, such as lapatinib, which inhibits HER2 and EGFR, and vandetanib, which

* Corresponding author.Center for Cancer Research, Medical University of Vienna, Borschkegasse 8a, A-1090, Vienna.
E-mail address: petra.heffeter@meduniwien.ac.at (P. Heffeter).
[1] these authors contributed equally to the main findings of the manuscript.

https://doi.org/10.1016/j.canlet.2023.216237
Received 31 January 2023; Received in revised form 8 May 2023; Accepted 17 May 2023
Available online 19 May 2023

inhibits in addition to EGFR also the vascular endothelial growth factor receptor (VEGFR) and the RET-tyrosine kinase [9]. However, besides drug resistance, especially occurrence of adverse effects is a major limitation of all EGFR-targeted therapeutics. The reason is that the EGFR has a physiologically important function in skin development and, thus, papulopustular rash is frequently observed in patients treated with EGFR inhibitors [9]. Most importantly, there is a direct correlation between the severity of the rash and the response to therapy [10,11]. Consequently, especially those patients who would profit most from EGFR-inhibitory therapy have to stop treatment due to adverse effects. Since a few years, osimertinib is used as first-line therapy, which is better tolerable than the 1st or 2nd line EGFR-TKIs. However, still about 25% of the patients experience severe treatment-related toxicities [12] and relapse based on resistance development is eventually observed in all patients [13] with only limited options for second-line therapy [13]. In fact, there are now considerations to start therapy with a 1st or 2nd line EGFR-TKI, followed by osimertinib upon relapse which would lead to a longer overall survival of the patients [14]. Noteworthy, 1st or 2nd line EGFR-TKIs (such as erlotinib) are usually not applied as monotherapies but in drug combinations, often with the *anti*-VEGF antibody bevacizumab. Also combination with small molecule VEGFR inhibitors such as sunitinib has been clinically investigated. However, these combinations were limited by severe synergistic toxicities [15,16]. To overcome these problems, we have developed a new cobalt(III)-based EGFR inhibitor prodrug system, which is specifically activated in the hypoxic areas of the malignant tissue [17]. In more detail, the prodrug was designed using a new EGFR-inhibitor molecule (KP2187, Fig. 1A) bound to cobalt(III), forming a very stable complex. This complex, named KP2334, is too bulky to interact with the EGFR under normal physiological conditions. In the specific hypoxic conditions of the solid tumor tissue, the prodrug is reduced to its respective cobalt(II) complex resulting in release of KP2187 in a highly tumor-specific manner. The promising anticancer activity of this new prodrug concept has been shown making KP2334 an interesting candidate for further preclinical development towards a first-in-man clinical phase I trial [17,18]. However, as KP2187 is a new EGFR-inhibitory molecule, its exact mode of action still needs to be fully characterized and the impact of diverse common EGFR inhibitor resistance mechanisms evaluated to allow the selection of an appropriate patient collective. This is especially of importance as KP2187 has a chelating moiety, which could lead to formation of complexes with endogenous metals potentially interfering with its EGFR-binding properties. Consequently, aim of the here

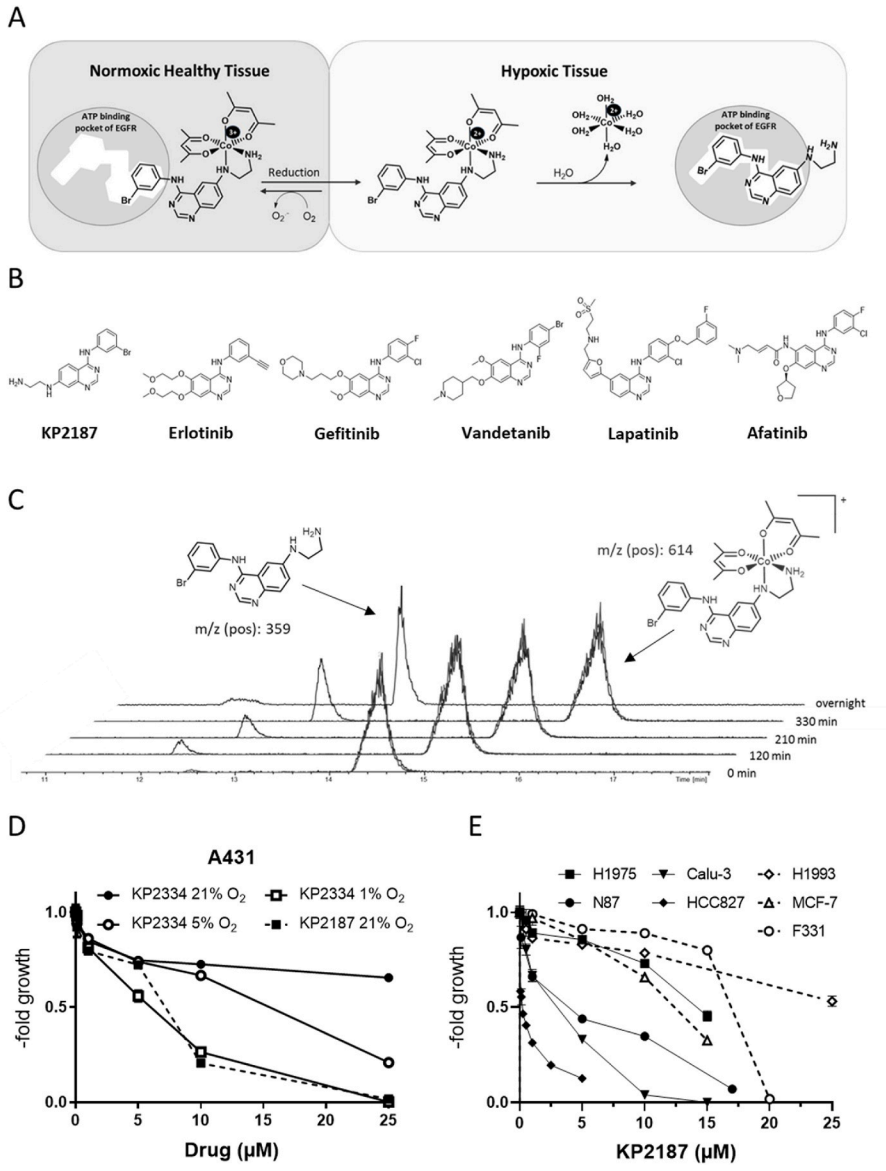

Fig. 1. Hypoxic activation of KP2334 and release of KP2187. (A) Proposed mode of action of KP2334 based on the reduction of Co(III) to Co(II) in the hypoxic tumor tissue followed by the release and EGFR binding of the biologically active ligand KP2187. (B) EGFR inhibitors used in this study; (C) Ligand release kinetics of KP2187 from KP2334 measured by HPLC and mass spectrometry after the indicated time points (D) Cytotoxic activity of KP2334 and KP2187 against wild-type EGFR-overexpressing A431 cancer cells was tested by MTT viability assays. Incubation time of the compounds on the cells was 72 h under normoxic (21% O_2) or hypoxic conditions (1% or 5% O_2). (E) Dose-response curves of KP2187 in the indicated erlotinib-sensitive (HCC827, Calu-3 and N87) and -resistant cell models (H1650, MCF-7, H1993 and F331) after 72 h. Values from all viability assays are given as means ± SD of one representative experiment performed in triplicates.

presented study was to further investigate the biological activity of this new small molecule not only with regard to its mode of action but also in comparison to five clinically approved drugs with known inhibitory activity of the EGFR in its wild-type or mutationally activated state: erlotinib, gefitinib, vandetanib, lapatinib and afatinib (Fig. 1B). This makes our prodrug strategy especially relevant for therapy settings where wild-type EGFR activation mediates treatment failure and combination approaches are frequently limited by enhanced toxicity.

2. Material and methods

2.1. Chemicals

KP2334 and KP2187 were synthesized as previously described [17]. Erlotinib hydrochloride, gefitinib (free base), lapatinib di-p-toluenesulfonate, vandetanib (free base), afatinib (free base), sunitinib malate salt, ponatinib (free base), sorafenib p-toluoenesulfonate and axitinib (free base) were purchased from LC laboratories. Osimertinib mesylate was from MedChemExpress. For cell culture studies all TKIs were dissolved in DMSO (10 mM stocks) and stocks stored at −20 °C. For the experiments, stocks were diluted in cell culture medium (DMSO concentrations were always <1%).

2.2. KP2187 release kinetics

Phosphate-buffered saline (PBS) (pH 7.4) containing 5 μM KP2334 was incubated at 20 °C under inert conditions (argon atmosphere) and 100 eq. of the reducing agent dithiothreitol were added. The reduction process was monitored on an Agilent 1260 Infinity system with a Waters Atlantis T3 column (2.1 × 150 mm) coupled to a Bruker amaZon SL ESI-IT mass spectrometer. Milli-Q water, containing 0.1% formic acid, and acetonitrile containing 0.1% formic acid were used as eluents. A gradient of 1–99% in 29 min was applied. The peak at 11.5 min belongs to KP2187 after release from KP2334 at 14.5 min (the m/z = 359 signal at 14.5 min corresponds to a KP2187 artefact which is formed inside the mass spectrometry).

2.3. Docking

Molecular docking was performed using AutoDock 4.2 [19]. The Protein Data Bank files PDB id: 4G5J and PDB ID: 4G5P were used as models for EGFR (wild type and mutated, respectively) in complex with afatinib. Autodock Tools 1.5.6 software was used to remove water and ligand molecules and to add hydrogens and Gasteiger charges to the selected receptors [19]. In order to be used for docking studies, the structures of erlotinib, gefitinib, vandetanib, lapatinib, afatinib and KP2187 were fully optimized by DFT calculations implemented in the Gaussian09 program package [20], using the B3LYP functional [21], and the 6-311G* basis set.

For the docking calculations, a grid box sufficiently large to include the binding pocket of the protein and possible ligand-receptor complexes was created. In particular, the grid size was set to 100 × 100 × 100 points with grid spacing of 0.375 Å for both receptors. The grid centers were calculated according to the center of mass of afatinib in the two proteins: 50.68, 1.374 and −21.036 for 4G5J, and −10.922, 19.113 and 31.245 for 4G5P. Docking was run using the Lamarckian Genetic Algorithm with all the parameters set to default values. Estimated free energies of binding are expressed in kcal/mol. 2D interaction models were generated using LigPlot and its respective software [22]. Docking results were visualized using Chimera [23] and Pymol (L. Schrödinger, PyMOL Molecular Graphics System, version 1.8; Schrödinger: New York, 2015) softwares.

2.4. Cell culture

Detailed information as well as culture and MTT seeding conditions for used cell lines are provided in Suppl. Table 1. All cells were grown under standard cell culture conditions and regularly checked for mycoplasma contamination. The medium was supplemented with 10% fetal bovine calf serum (FBS) (purchased from PAA Linz, Austria). The TKI-resistant HCC827 cell models were continuously selected with the drugs indicated.

2.5. Selection of novel HCC827 clones with acquired TKI resistance

HCC827 cells were selected with two different EGFR TKIs, erlotinib and gefitinib. To select TKI-resistant cell clones the parental cells received either 20 μM erlotinib or 20 μM gefitinib once a month. The resistance of the cell models was checked by cell viability assays following 72 h drug treatment with increasing concentrations. Furthermore, the resistant cell models HCC827/Erlo and HCC827/Gefi were tested in a combination treatment with crizotinib to prove their c-Met dependence.

2.6. aCGH analysis

The DNA for Array CGH (aCGH) was isolated using the QIAamp DNA Blood Mini Kit (Qiagen) following the manufacturer's protocol. aCGH was performed using 2 × 400 K whole genome oligonucleotide-based arrays (Agilent Cancer Research Array + SNP, # G5956A). Labelling and hybridization procedures were performed according to the instructions provided by Agilent using the SureTag DNA Labelling Kit and the "Agilent Oligonucleotide Array-Based CGH for Genomic DNA Analysis" protocol. 500 ng of tumor DNA and reference DNA (human male genomic DNA, Promega) were digested with AluI and RsaI, and labelled by random priming with Cyanine 5- and Cyanine 3-dUTP, respectively. After purification, the Blocking agent, Hybridization Buffer (Oligo aCGH/Chip-on-Chip Hybridization Kit, Agilent) and cot-DNA (Roche), were added to the labelled samples and the whole suspension hybridized onto oligonucleotide arrays. In case of indirect aCGH, the respective parental cell line was used as a reference DNA. The hybridization was carried out for 48 h at 67 °C in a hybridization oven (Agilent). The slides were scanned with a G2600D Microarray Scanner (Agilent). Feature extraction and data analysis were carried out using the Feature Extraction (version 10.7.3.1) and Agilent Genomic Workbench software (version 7), respectively.

2.7. Cell viability assays

Cells were plated (depending on the cell model 2–7x 10^3 cells/well) in 96-well plates and allowed to recover for 24 h. Subsequently, the indicated drugs or their combinations were added. In case of the hypoxia experiments, a hypoxia chamber (c-chamber equipped with a ProOxC21O_2/CO_2Controller from Biospherix NY, USA) at 1% O_2/5% CO_2 level was used. After 72 h exposure, the proportion of viable cells was determined by MTT assay following the manufacturer's recommendations (EZ4U kit, Biomedica). Cytotoxicity was expressed as IC_{50} values calculated from full dose-response curves using Graph Pad Prism 8 software.

Table 1
Docking free energies of binding with wild-type EGFR (PDB: 4G5J).

Drugs	EGFR/wt (Autodock)
Afatinib (seed)	−8.09
KP2187 (position 1)	−6.99
KP2187 (position 2[a])	−8.13[a]
Erlotinib	−6.86
Gefitinib	−6.83
Lapatinib	−7.71[a]
Vandetanib	−7.36[a]

[a] No overlap with afatinib classic pose.

2.8. Western blot analysis

To assess the impact of the drugs on the EGFR signaling pathway, A431 cells were starved by serum deprivation for 24 h before treatment to reduce the impact of other tyrosine kinase receptors like PDGFR or VEGFR. Then cells were incubated with the drugs for 4 h (2.5 and 5 μM). To assure EGF-dependent activation of the signaling pathway, EGFR stimulation was induced 10 min before protein isolation with 50 ng/ml EGF. Total protein lysates or membrane-enriched extracts (of untreated cells) were prepared, separated by SDS-PAGE, and transferred onto a polyvinylidene difluoride membrane for Western blotting as described previously [24]. Primary antibodies used in this study are given in Suppl. Table 2. Secondary, horseradish peroxidase-labelled antibodies from Santa Cruz Biotechnology were used in working dilutions of 1:10 000.

2.9. Annexin V-/PI-staining

2×10^5 cells/well were seeded in 6-well plates. After overnight recovery, the cells were treated for 24 h with the indicated drug concentrations. For staining with annexin V-APC (AV) and propidium iodide (PI) the medium as well as the trypsinized cells were harvested. Fluorescence intensity was measured by flow cytometry using a FACS Calibur (Becton Dickinson, Palo Alto, CA) and quantified by FlowJo software (version 10.1).

2.10. Animals

Eight-twelve week-old C.B.17 SCID mice were purchased from Envigo, Italy. The animals were kept in a pathogen-free environment and every procedure was done in a laminar airflow cabinet. Experiments were done according to the regulations of the Ethics Committee for the Care and Use of Laboratory Animals at the Medical University Vienna (proposal number BMWF-66.009/0081-WF/V/3b/2015), the U.S. Public Health Service Policy on Human Care and Use of Laboratory Animals as well as the United Kingdom Coordinating Committee on Cancer Prevention Research's Guidelines for the Welfare of Animals in Experimental Neoplasia. To ensure animal welfare throughout the experiment, the body weight of the mice was assessed once a day.

2.11. Xenograft experiments

For therapy experiments, A431, PC-9 and Calu3 cells (1×10^6) were injected subcutaneously into the right flank of the mice. Animals were randomly assigned to treatment groups and therapy was started when tumor nodules were palpable. Animals were treated intraperitoneally (i.p). with 25 mg/kg KP2187 (dissolved in 0.9% NaCl) at 5 consecutive days/ week for two weeks. Animals in the control group received 0.9% NaCl (i.p.) only. In the combination experiment of KP2187 with sunitinib (or bevacizumab), KP2187 treatment (i.p.) was given in combination with oral applications of sunitinib (40 mg/kg dissolved in 10% DMSO in citrate puffer pH 3.5) or i.p. treatment with bevacizumab (5 mg/kg dissolved in PBS) on the indicated days. Animals were monitored for distress development every day and tumor size was assessed regularly by caliper measurement. Tumor volume was calculated using the formula: (length $\times$ width^2)/2. On the last day of the experiment, animals were sacrificed by cervical dislocation and tumors collected for fixation in 4% formaldehyde for 24 h (Carl Roth) followed by paraffin embedding using a KOS machine (Milestone). For histological evaluation, tumor tissues were sliced in 4 μm thick sections and hematoxylin/eosin stained by routine procedures.

2.12. Immunohistochemistry

Fresh sections were deparaffinized and dehydrated. In brief, after antigen retrieval by boiling for 30 min in 10 mM citrate buffer (pH 6.0), sections were incubated with a pERK (Tyr202/Tyr204, Cell Signaling, 1:400) or pEGFR-specific antibody (Tyr1068, Cell signaling, 1:200) in a humid chamber for 1 h at room temperature. In case of the Ki67 antibody (Dako, 1:100), a 30 min incubation was sufficient. Antibody binding was detected using the UltraVision LP detection system according to the manufacturer's instructions (Thermo Fisher Scientific Inc.). Color was developed using 3,3′-diaminobenzidine (Dako). Pictures of stained slides were taken with a Nikon Eclipse 80i microscope, together with a DS-U3 control unit and the adequate NIS-Elements software (all from Nikon Instruments). Evaluation and quantification of the staining was done by Definiens software.

2.13. Statistic and calculation of correlation

In general, the statistical analyses were performed using GraphPad PRISM 8 or R version 4.0.4 (2021-02-15) [25]. Differences between two groups were determined by using Welch's *t*-test when applicable. To get first indications for potential correlations, Western blots were quantified with FIJI software and corrected to the respective β-actin loading controls (Suppl. Table S3). Expression levels were grouped into no (0), low (1), mediate (2) and high (3). For the calculation, the linear regression analysis tool of the GraphPad PRISM 8 software was used. Subsequently, the collected data was evaluated by linear regression to estimate a model between the independent variable IC_{50} and the data summarized in Table S4 as dependent variables. For linear regression analysis, the R-package MASS in the version 7.3–53.1 [26] was applied. A step-wise feature reduction was performed.

3. Results

3.1. The Co(III) complex KP2334 releases the novel EGFR inhibitor KP2187 under hypoxic conditions

As described above, we recently designed the novel hypoxia-activatable EGFR prodrug KP2334 [17]. So far, hypoxic release of the EGFR-inhibitory ligand KP2187 from KP2334 was only indicated indirectly by fluorescence microscopy in living cells. In order to confirm that reduction of the cobalt(III) prodrug indeed leads solely to KP2187 release, HPLC and mass spectrometry experiments were performed. The ligand release kinetics are shown in Fig. 1C, proving evidence for specific KP2187 liberation from the complex. With regard to its biological effects, KP2334 has strong anticancer activity against EGFR-overexpressing cells such as A431 (erlotinib-sensitive, EGFR wild-type) in hypoxia-dependent manner (Fig. 1D). Noteworthy, only under severe hypoxic conditions (1% O_2) full anticancer activity comparable to free KP2187 was observed, indicating that the complex is also widely stable under weak hypoxic conditions, which is important for its tumor selectivity (Fig. 1D). Hypoxia has no impact on the activity on KP2187 itself or other commercially available EGFR inhibitors (Suppl. Fig. S1). In contrast to EGFR-dependent cell models such as the lung cancer cells (HCC827, Calu-3, N87), cells which grow in an EGFR-independent manner, such as the lung carcinoma H1993 (a c-Met-dependent model [27]), the breast cancer model MCF-7 (which does not express EGFR), or human F331 fibroblasts did not respond to KP2187 (Fig. 1E). In addition, also cells with a T750M mutation in the EGFR (H1975) were insensitive to KP2187 (Fig. 1E).

3.2. Anticancer activity and EGFR inhibition of KP2187 in vivo and in cell culture

In order to allow the development of KP2334 towards clinical studies, a detailed understanding of the released bioactive ligand (KP2187) *in vitro* and *in vivo* is necessary. This is especially relevant as KP2187 harbors an ethylenediamine moiety with metal-chelating properties, which could interfere with its desired biological behavior. Cell-free kinase activity assays already showed that KP2187 has potent

EGFR-inhibitory potential (IC_{50} values of 0.95 nM against wild-type EGFR), which is even stronger than that of erlotinib [17]. Accordingly, also in A431 xenografts strong inhibition of the EGFR-signaling pathway was observed after KP2187 treatment (Fig. 2A). This resulted in distinct anticancer activity of KP2187 against EGFR-dependent cell models such as A431, Calu-3 and PC-9 *in vivo* (Fig. 2B and C). Subsequently, histological analysis of A431 tumors revealed that this activity was based mainly on cell cycle arrest and not on apoptosis (Fig. 2D). This was highlighted by a significant reduction of Ki-67 positive cells in the tumor already after 24 h (Fig. 2E), while no indications for increased (apoptotic) cleavage of caspase-3 were found.

To gain further insight into the impact of KP2187 on the EGFR-signaling pathway, phosphorylation of different EGFR tyrosine residues as well as down-stream ERK, AKT and S6 were investigated by Western blotting in cell culture experiments. In these assays, KP2187 was evaluated in comparison to five other clinically approved TKIs with known EGFR-inhibitory potential, namely erlotinib, gefitinib, vandetanib, lapatinib and afatinib (compare Fig. 1B). As expected, all compounds were able to inhibit EGF-induced signaling in serum-starved A431 cells (Fig. 3A). However, distinct differences regarding the individual impact on the EGFR-downstream pathways were observed. In more detail, KP2187 mainly resembled erlotinib with strong inhibition of EGFR phosphorylation of Tyr1068 and Tyr992 (while not affecting Tyr1045) together with strong impact on downstream signaling pathways (pERK, pAKT, pS6). In contrast, especially vandetanib and lapatinib showed a distinctly different picture: thus, they had weak impact on phosphorylation of the three tested EGFR tyrosine residues, and only reduction of pAKT and pS6, but not pERK was observed. This indicates that there are differences in the interaction of these compounds with the EGFR molecule.

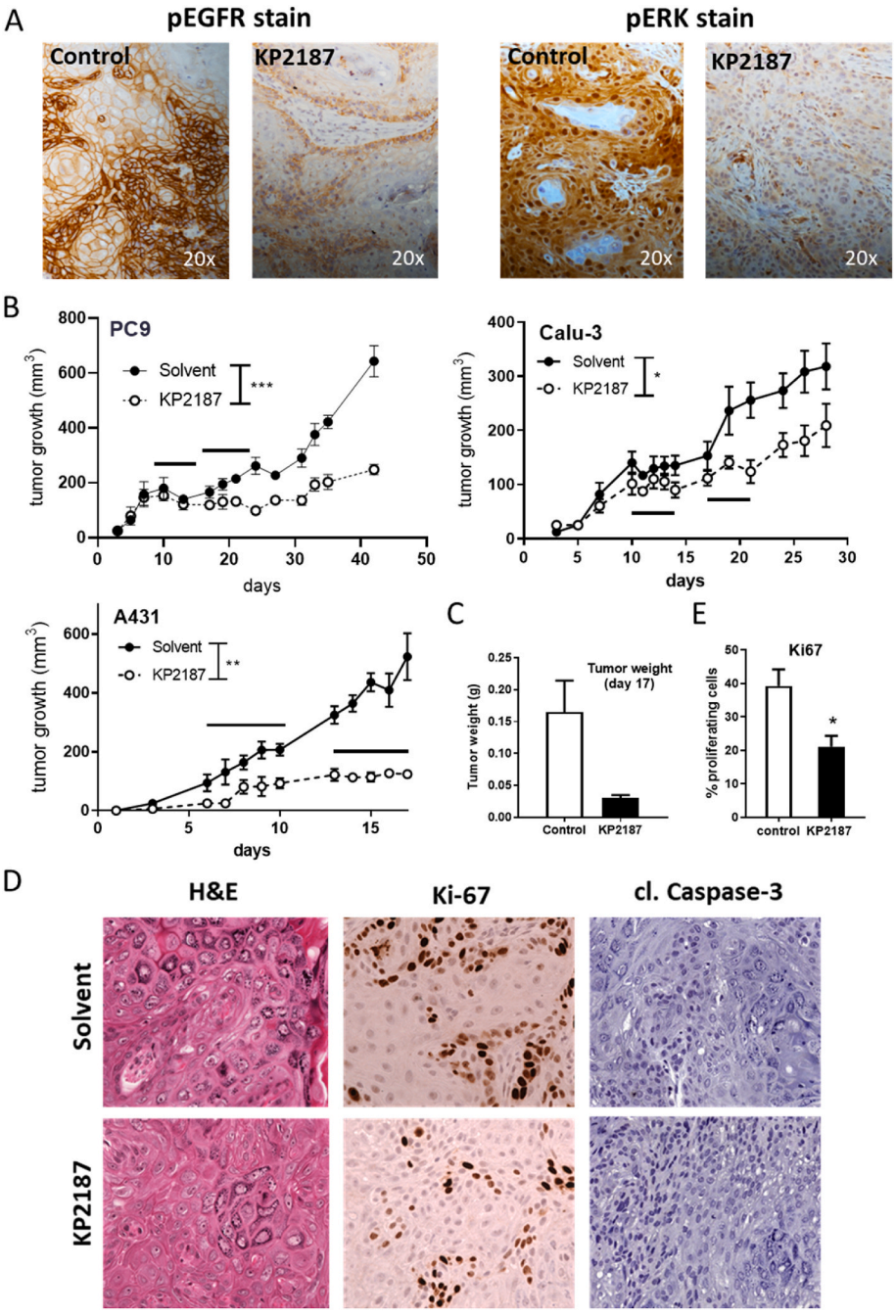

Fig. 2. Anticancer activity of KP2187 *in vivo*. C.B.17Scid/scid mice were inoculated subcutaneously (s.c.) with the respective cancer cells at the right flank and treated with 25 mg/kg KP2187 (i.p.) for 5 consecutive days for 2 weeks, when measurable tumors had formed. (A) pEGFR and pERK expression levels in paraffin-embedded and formalin-fixed A431 tumors 24 h after therapy. (B) Impact of KP2187 therapy on PC-9, Calu3 or A431 tumor growth. Data are presented as means ± SEM. Statistical significance was tested by two-way ANOVA (* $p < 0.05$, ** $p < 0.01$, ***$p < 0.001$). On the last day of therapy, A431 tumors were collected, formalin-fixed, paraffin-embedded and analyzed for diverse histological parameters. (C) Impact of KP2187 treatment on tumor weight at section (mean± SD). Statistical significance was analyzed by unpaired *t*-test (**$p < 0.01$). (D) Representative images for the H&E (general morphology), Ki-67 (proliferation marker), cl. caspase-3 (apoptosis marker) stains of the A431 tumors are shown. (E) Quantification of the Ki-67 stains by Definiens software. Statistical significance was analyzed by unpaired *t*-test (*$p < 0.05$).

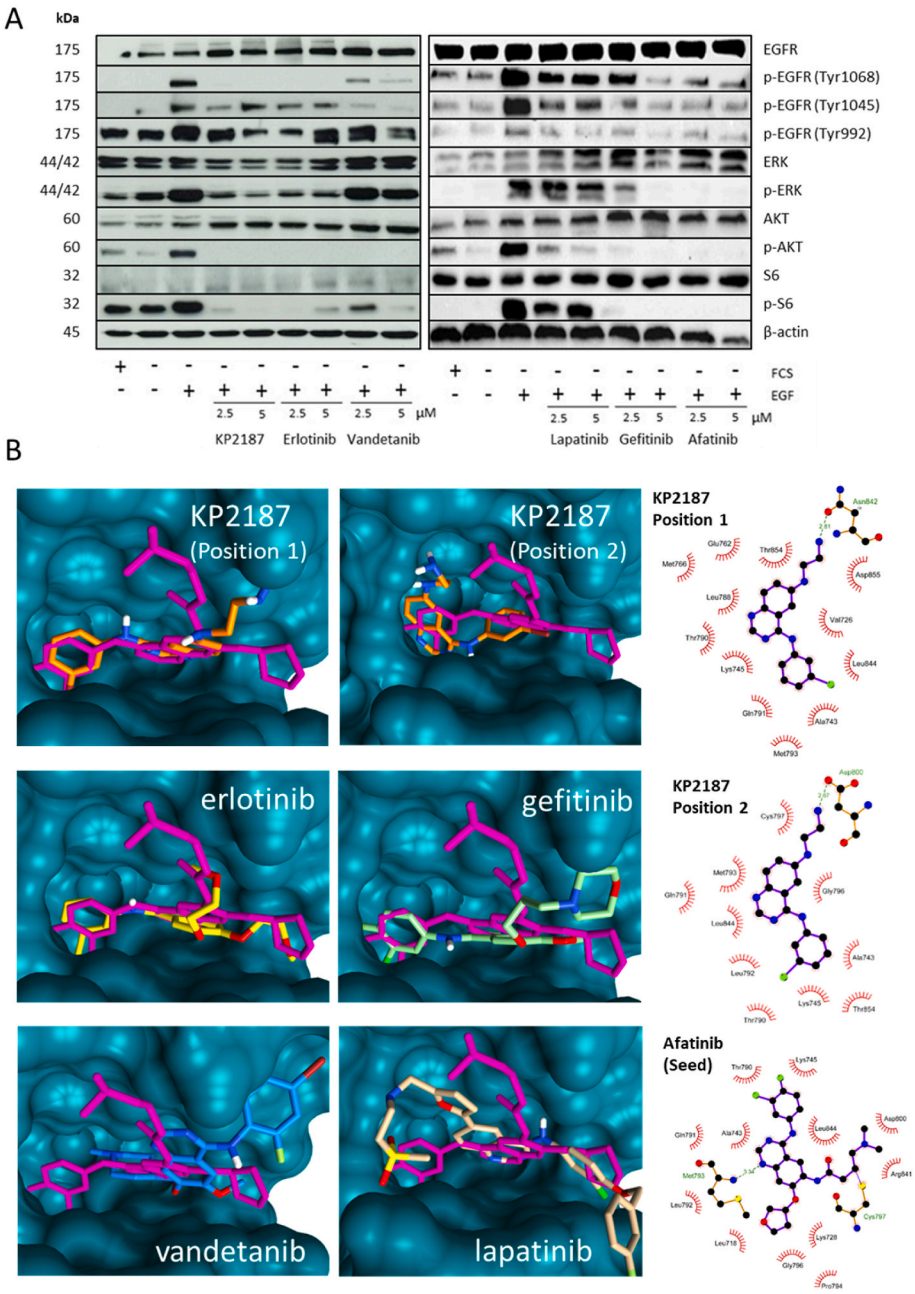

Fig. 3. EGFR-inhibitory potential of KP2187 compared to different approved EGFR inhibitors. (A) Inhibition of EGFR phosphorylation and downstream signaling pathways. A431 cells were grown in medium with or without FCS and treated with the indicated drug for 4 h. After EGFR stimulation with 50 ng/ml EGF for 10 min, cells were harvested, lysed and total protein extracts were collected for Western blot analysis. β-actin served as loading control. (B) Left panel: 3D representation of the best poses obtained by molecular docking performed using AutoDock 4.2. The crystal structures of afatinib bound to human wild-type EGFR (PDB id: 4G5J) were used after removing afatinib (indicated in pink) from the respective proteins. All ligands were docked to the ATP-binding pocket of the EGFR molecule with KP2187 depictured in two different positions. Right panel: schematic 2D diagrams of protein–ligand interactions for wild-type EGFR in complex with KP2187 in the two different positions and with afatinib. Hydrogen bonds are indicated by dashed lines, while hydrophobic contacts are represented by an arc with spokes radiating toward the ligand atoms they contact. The contacted atoms are shown with spokes radiating back. No spatial information can be inferred from the 2D diagrams.

3.3. Differences in the EGFR-binding between KP2187 and the other EGFR inhibitors in silico

To investigate whether the compounds indeed have a different interaction profile with the ATP-binding pocket of the EGFR molecule, docking studies were performed. To this end, the crystal structure of afatinib bound to human wild-type EGFR (PDB id: 4G5J) was used as starting model (Suppl. Fig. S2). Afatinib was then removed from the respective protein and all ligands were docked to the EGFR pocket. With regard to KP2187 (Fig. 3B), two different possible orientations inside the ATP-binding pocket were found: one in which the inhibitor is oriented like afatinib (Fig. 3B, position 1) and a second in which KP2187 is almost turned by 180° with its bromophenyl group out of the pocket (Fig. 3B, position 2). The 2D schematic diagrams of protein–ligand interactions of Fig. 3B show how KP2187, when in position 1, is surrounded by the same amino-acidic residues of afatinib, while this is clearly not the case when it is in position 2. The binding of both orientations was very strong, with position 2 having even stronger binding affinity to the EGFR molecule than afatinib itself when re-docked (Table 1). Concerning the other inhibitors, erlotinib and gefitinib could be fitted into the EGFR in an orientation comparable to afatinib, while lapatinib and vandetanib had distinctly other preferential orientations (which also interfered with their proper binding into the EGFR pocket) (Fig. 3B and Suppl. Fig. S3). These differences in fitting into the ATP-binding pocket are well in agreement with the Western blot experiments and could serve as a good explanation why lapatinib and vandetanib had a different EGFR-downstream signaling inhibition pattern (compare Fig. 3A). Noteworthy, as the afatinib conformation was used as starting point for the modeling, it is not surprising that the calculated free energy values of all other drugs were lower than afatinib (except position 2 of KP2187). However, the gained values still indicate strong binding potential to the wild-type EGFR (Table 1).

3.4. Correlation of KP2187 activity with other TKIs and impact of receptor tyrosine kinase expression and EGFR inhibitor resistance mechanisms

In order to investigate whether the anticancer activity of KP2187 biologically correlates with the approved TKIs used in this study, a panel of 24 cancer cell lines was tested for their sensitivity by MTT viability assays after 72 h (Suppl. Table S5). In general, the anticancer activity profile of KP2187 strongly and significantly correlated especially with the one of gefitinib and lapatinib with r-values of 0.86 and 0.89, respectively (Suppl. Fig. S4). Noteworthy, in case of erlotinib, no IC_{50} values were reached in some cell lines due to the poor water solubility of this drug, which did not allow testing concentrations >25 μM. Consequently, only an r-value of 0.74 was found, which was also in the range of the multi-kinase inhibitor vandetanib. The correlation with afatinib was lowest but significant with 0.62. Interestingly, a preliminary correlation of KP2187 with osimertinib activity revealed no significance with an r-value of only 0.51. However, it has to be mentioned that only a limited number of cell lines was tested with osimertinib (n = 9).

As a next step, we evaluated whether the expression levels of total EGFR could be used as a marker for responsiveness to KP2187. To this end, the expression levels of total EGFR were quantified by Western blotting of membrane-enriched protein fractions (Fig. 4A). Based on the strong similarity of the KP2187 profile with the other EGFR inhibitors, it is interesting that no correlation of KP2187 activity with the EGFR expression levels was found (r-value of 0.36, Fig. 4B). Also when analyzing the basal activity of the EGFR-downstream signaling, no significant correlation with any of the EGFR inhibitors could be observed (data not shown). Notably, similar observations have been reported in literature e.g. for erlotinib [28–30], which could be confirmed also with

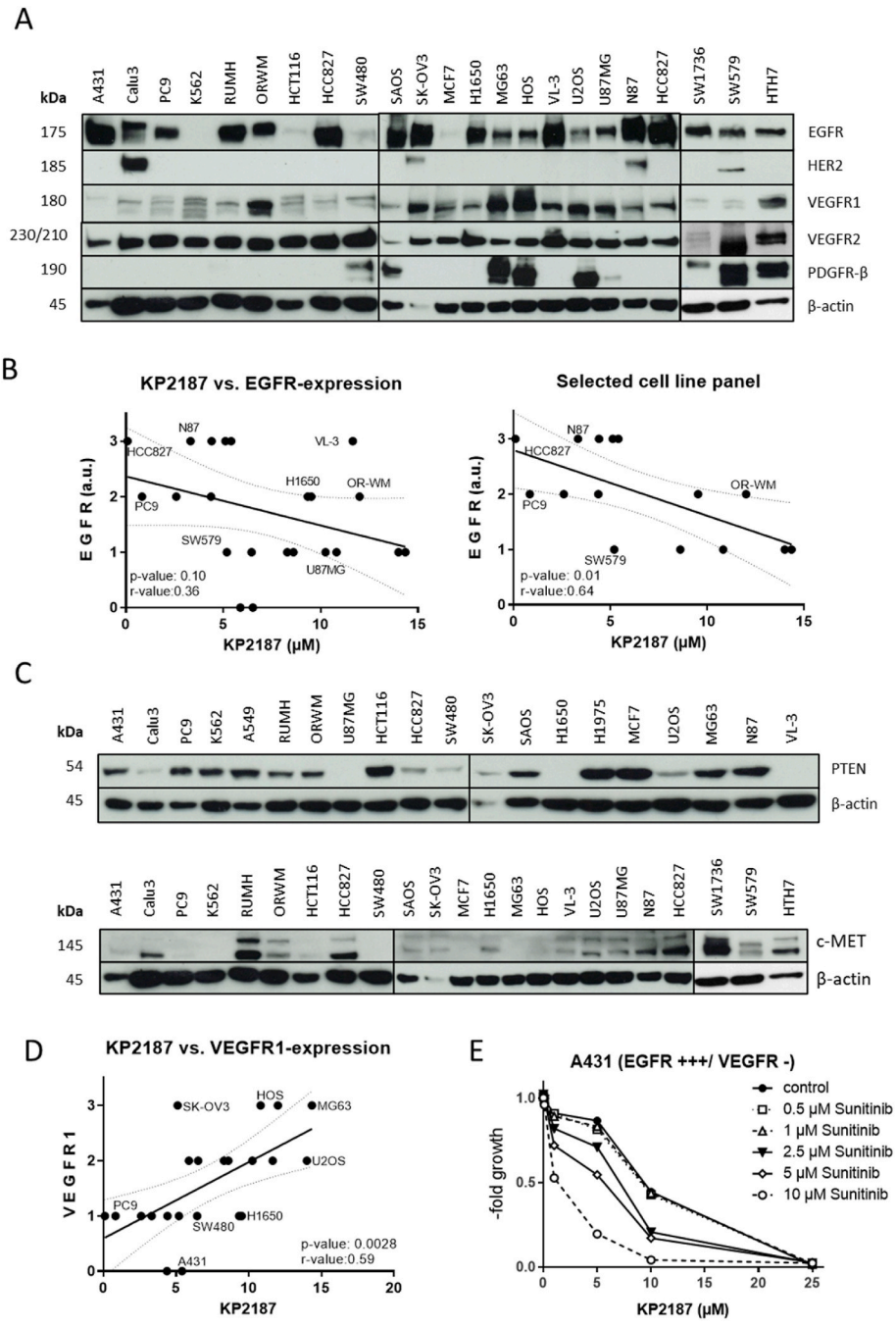

Fig. 4. Correlation of KP2187 activity with expression of diverse RTKs and factors leading to EGFR inhibitor resistance. (A) RTK expression levels of various cancer cell lines. Protein lysates of membrane-enriched fractions were used for Western blot analysis. β-actin served as loading control. (B) Correlation of KP2187 IC_{50} (μM) values of different cell models with their EGFR expression levels which were determined by Western blot analysis. Correlation was calculated with a linear regression model using GraphPad Prism 8 Software. (C) Expression levels of PTEN and c-Met of different cancer cell models measured by Western blot analysis from total protein extracts. β-actin served as loading control. (D) Correlation of KP2187 IC_{50} (μM) values of different cell models with their VEGFR1 expression. Correlation was calculated with a linear regression model using GraphPad Prism 8 Software. (E) Synergistic effects of KP2187 with sunitinib in A431 cells. Cells were co-treated with both drugs at the indicated concentrations for 72 h. Cytotoxic effect was measured using an MTT-based assay. Values are given as means ± SD of one representative experiment performed in triplicates.

our data (Suppl. Fig. S5). Hypothesizing that the weak correlation with the EGFR expression levels might be based on other factors influencing the sensitivity to EGFR inhibition, we validated diverse other characteristics, which were reported to render cells unresponsive to EGFR inhibitors (Fig. 4C). Thus, we performed a step-wise exclusion of cells with PTEN deletion (U87MG, H1650, VL-3), c-Met overexpression (RU-MH, SW1736) as well as KRAS mutation (SW480, HCT116). In addition, the two EGFR/null cell lines MCF-7 and K652 were excluded. By considering PTEN deletion and KRAS mutation, we could distinctly improve the correlation between the EGFR expression levels and KP2187 activity to a significant r-value of 0.64. Interestingly, exclusion of c-Met-overexpressing lines had no positive impact on the correlation. This indicates that PTEN loss and KRAS mutation could be (comparable to other EGFR TKIs) also biomarkers for KP2187 resistance. In order to further evaluate, whether mechanisms associated with resistance to erlotinib and gefitinib also impact on KP2187 activity, isogenic HCC827 subclones with acquired erlotinib/gefitinib resistance were used. Two models overexpressing c-Met (HCC827/erlo and HCC827/gefi) were established in our lab by continuous exposure to erlotinib and gefitinib, respectively. C-Met expression in these models is based on gene amplification and was confirmed by Western blotting as well as sensitivity to the c-Met inhibitor crizotinib in cell viability assays (Suppl. Fig. S6). As a third subline HCC827/EPR cells were used, which were co-selected by erlotinib and the c-Met inhibitor PHA-665752 and harbor the secondary acquired T790M mutation [31]. Comparable to erlotinib and gefitinib, all three HCC827 submodels have strong cross-resistance to KP2187 (Suppl. Fig. S7), which is in line with the hypothesis that the chelating moiety does not interfere with the EGFR-binding properties of our new drug.

We also evaluated our cell line panel for the expression of other receptor tyrosine kinases (RTKs), namely HER2, VEGFR1/2, and PDGFR-β (Fig. 4A). In case of HER2, only 4 positive cell models were found (Calu3, HTB77, N87, SW578). Thus, although there are indications for HER2 expression rendering cells more sensitive to KP2187, no statistical significance for this observation was reached due to the limited number of cell models positive for this RTK (Suppl. Fig. S8). This suggests the need of more in-depth studies to dissect HER2 as positive marker for KP2187 activity. Furthermore, no significant impact of PDGFR-β and VEGFR2 expression levels on KP2187 was detected (Suppl. Figs. S9 and S10). In contrast, for VEGFR1 a highly significant positive correlation between expression levels and KP2187 IC_{50} values was found (Suppl. Fig. S11), indicating that VEGFR1 could be a resistance factor. To process the amount of collected data (Suppl. Table S4) in a more comprehensive manner, further mathematical analyses were performed. In a first step, we included all features as independent variables. We could observe that indeed VEGFR1 had a significant independent effect ($p < 0.01$) on IC_{50} values, while this was not the case for all other variables analyzed. As a second step, we performed a stepwise backwards elimination approach by removing all independent variables not associated with IC_{50} values of KP2187 and re-performed the calculation. The association between VEGFR1 and IC_{50} values remained significant ($p < 0.01$). Consequently, we got interested, whether inhibition of VEGFR was able to enhance the activity of KP2187.

3.5. Synergism of KP2187 with diverse VEGFR inhibitors in vitro and in vivo

Due to the positive correlation of VEGFR1 expression with the IC_{50} values of KP2187, we hypothesized that simultaneous administration of KP2187 with VEGFR inhibitors has synergistic effects. Indeed, co-treatment of cancer cells with KP2187 and the pan-VEGFR inhibitor sunitinib for 72 h revealed a striking synergism in several models (Fig. 4E and Suppl. Fig. S12). This was also true for other VEGFR inhibitors such as axitinib, sorafenib, and ponatinib (Suppl. Fig. S13) and independent of the basal EGFR and VEGFR expression levels (Fig. 4E and Suppl. Fig. S12). Noteworthy, the combination was also very efficiently able to break the KP2187 resistance based on T790M mutation (in H1975 cells) or PTEN loss (in H1650 cells) (Suppl. Fig. S12)

To investigate, whether this also translates into the *in vivo* situation, A431 xenograft experiments were performed. The treatment was applied once daily for two weeks on 5 consecutive days with either KP2187, sunitinib as monotherapy or a combination of KP2187 with sunitinib. The combination was well tolerated, with less than 10% loss in body weight over the course of therapy (Suppl. Fig. S14). KP2187 and sunitinib mono-treatment both significantly reduced tumor growth ($p < 0.05$ and $p < 0.001$), respectively after the end of therapy calculated by 2way ANOVA (Fig. 5A) and thus, prolonged overall survival of the animals (from 25 days in solvent control to 31 and 32 days, respectively, Suppl. Fig S15). However, the combination treatment was distinctly and significantly superior to the monotherapies ($p < 0.05$ and $p < 0.01$, respectively), resulting after initial remission in a complete blockade of tumor growth until end of therapy. Consequently, a mean overall survival of 40 days was reached, with one of the mice surviving about 40 days after stop of therapy (until day 60). Noteworthy, KP2187 also displayed a very strong synergism with the monoclonal *anti*-VEGF antibody bevacizumab against A431 tumors (Fig. 5B). To gain more insight into the underlying histological changes, a second experiment of the KP2187 combination with sunitinib was performed, where the tumors were collected on the last day of therapy (day 21), paraffin-embedded and formalin-fixed (tumor weights at section are shown in Suppl. Fig. S16). H/E stains already indicated that the tumors of the combination therapy were characterized by large necrotic areas (Fig. 5C). Subsequently, the tissues were stained for Ki-67 as marker for proliferation and cl. caspase-3 for apoptosis. In good agreement with the KP2187 experiment shown in Fig. 2, again the drug dramatically decreased the percentage of Ki-67-positive cells, while cl. caspase-3 remained unchanged. Furthermore, sunitinib reduced the Ki-67-positive cell fraction to some extent. Both drugs did not increase the percentage of apoptotic cells. In contrast, when analyzing the tumors of the combination treatment, we observed a strong staining for cl. caspase-3 especially at the borders to the large necrotic areas indicating a shift from cell cycle arrest to apoptotic cell death (Fig. 5D). Interestingly, when looking at the pEGFR levels, we discovered that sunitinib mono-therapy strongly stimulated the activation of this signaling pathway (Fig. 5C), which could explain the synergistic activity of the two drugs. In order to investigate, whether this effect is based on cellular interactions in the tumor microenvironment or is induced also on the cellular level, cell culture experiments with A431 cells were performed. Indeed, we could show that the drug combination led to a synergistic induction of apoptotic cell death (Fig. 5D and E). Moreover, Western blot experiments confirmed increased EGFR phosphorylation after sunitinib treatment (Suppl. Fig. S17). In contrast, total EGFR remained unchanged on both protein (Suppl. Fig. S17) as well as mRNA level (Suppl. Fig. S18).

4. Discussion

The development of novel TKIs against oncogenic signaling pathways is one of the most active research fields of modern cancer drug development. Consequently, besides kinase-targeting monoclonal antibodies, a large number of anticancer compounds, which were approved by the FDA within the last two decades, belong to the class of small-molecular kinase inhibitors targeting proteins involved in growth factor signaling, for example, the EGFR pathway [32–34]. However, despite their clinical success, problems with drug resistance and toxicity represent critical challenges in daily oncological routine [8,35]. Considering that monotherapy is rare in oncology, especially the identification of efficient target combinations is crucial and often hampered by enhanced combined toxicities, e.g. in case of EGFR inhibitors like erlotinib with VEGFR inhibitors such as sunitinib [15,16].

Most of the commonly used TKIs (including also erlotinib, gefitinib, lapatinib and vandetanib) target the ATP-binding pocket of the tyrosine

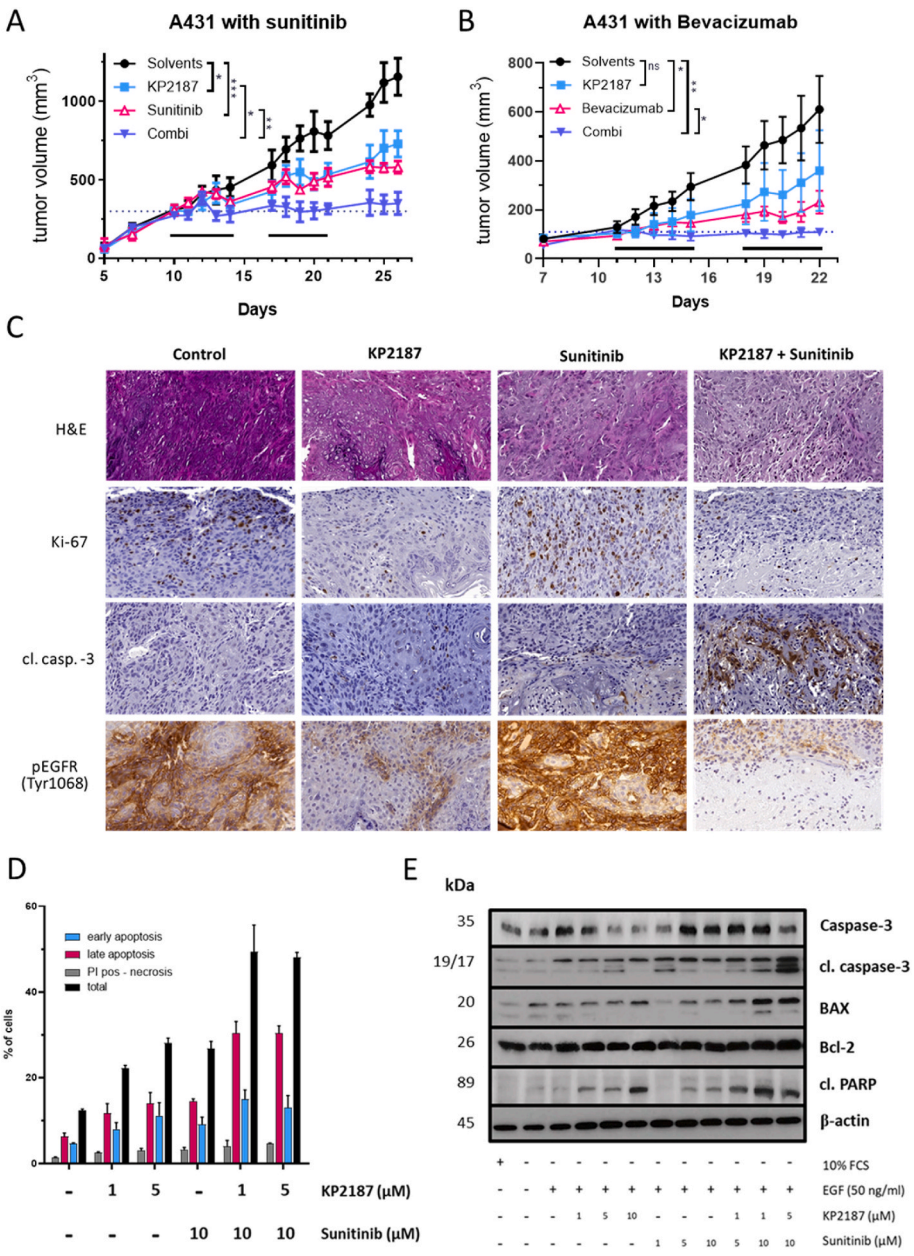

Fig. 5. Synergistic anticancer activity of KP2187 with sunitinib or bevacizumab. (A–C) A431-bearing C.B.17Scid/scid mice were treated once daily for two weeks on 5 consecutive days with KP2187 (14 mg/kg, i.p.), and sunitinib (40 mg/kg, per os (p.o.)) or bevacizumab (5 mg/kg i.p.) or their respective combinations. (A) Combination experiment with sunitinib; (B) Combination experiment with bevacizumab. Impact on tumor growth; data are presented as means ± SEM. Statistical significance was tested by two-way ANOVA (*$p < 0.05$, ** $p < 0.01$, ***$p < 0.001$). (C) In a second combination experiment with sunitinib, tumors were collected on day 21 (end of therapy) and sections were prepared for histological analysis (H&E stain) and immunohistochemically stained against Ki-67, cl. caspase-3, and pEGFR by using DAB and hematoxylin as counterstain. (D) Impact of KP2187, sunitinib and combination treatment on apoptosis induction in cell culture. A431 cells were treated with the indicated drug concentrations for 24 h and stained with annexin-V – APC and PI for apoptotic/necrotic cells. The amount of apoptotic cells was measured by flow cytometry. (E) Induction of cell death signaling upon drug treatment. A431 cells were grown in medium with or without FCS and treated with the indicated drug for 4 h. After EGFR stimulation with 50 ng/ml EGF for 10 min, cells were harvested, lysed and total protein extracts were collected for Western blot analysis. β-actin served as loading control.

kinase domain (also called type I inhibitors). In more detail, these drugs represent ATP competitors that bind to the molecule in its active conformation state [35]. This raises the opportunity for the development of prodrug systems, which are activated in a tumor-specific manner. In a former study, we designed a prodrug system, where a new EGFR inhibitor (KP2187) is stably bound to a cobalt(III) complex, which is too bulky to interact with the EGFR under normal physiological conditions [17]. Only in the hypoxic areas of the solid tumor tissue, the prodrug is activated to release KP2187 in a highly tumor-specific manner. However, in order to form a complex with the cobalt(III) molecule, specific structural adaptations (introduction of a ethylenediamine chelation moiety) of KP2187 were necessary. In this study, we were able to prove that this ethylenediamine moiety did not interfere with the EGFR-inhibitory potential of KP2187. In contrast, docking studies indicated that KP2187 binds very efficiently in "erlotinib" conformation into the ATP binding pocket of the EGFR. In addition, a potential second orientation, where the drug is 180° rotated, was predicted. Although these calculations have to be interpreted with caution, they are in line with cell-free kinase activity assays, which indicated that KP2187 could be an even more potent inhibitor of EGFR than erlotinib [17]. The subsequent biological studies in this manuscript confirmed that KP2187 is an efficient EGFR inhibitor with "erlotinib/gefitinib-like" effects on the EGFR-signaling pathway in cell culture as well as in xenograft models *in vivo*. Interestingly, also a strong correlation with the anticancer activity of the HER2/EGFR inhibitor lapatinib was observed, which together with the enhanced responsiveness of our four HER2-positive lines to KP2187 could indicate that HER2 is an additional target of our new EGFR inhibitor. This has to be followed up in future studies.

In the clinical routine, erlotinib is frequently combined with the *anti*-VEGF antibody bevacizumab [15]. Moreover, based on promising preclinical data, the combination of the EGFR inhibitor with the VEGFR1-3/PDGFR/c-kit inhibitor sunitinib was also evaluated up to a phase III clinical trial [36]. However, the combination has a rather narrow therapeutic window in humans hampering its successful clinical application [16]. As prodrug systems are a potent strategy to improve the tumor specificity of systemic cancer therapy, we were excited to see that also KP2187 has a strong synergistic anticancer activity with

sunitinib (and other clinically approved VEGFR inhibitors) in cell culture and *in vivo*. Noteworthy, the collected tumors revealed (besides enhanced apoptosis induction) large necrotic central areas in the combination treatment. Considering that it has already been published that a combination of afatinib with the VEGFR/PDGFR/FGFR inhibitor nintedanib resulted in reduced vascularization of the tumor tissue [37], this seems also likely for our drug combination. However, although a lot of clinical data exist, the exact mechanisms underlying the synergism are not fully understood.

VEGFR1 was initially believed to be expressed only on endothelial cells. However, recent studies, have demonstrated that VEGFR1 is also expressed on a variety of tumor cells [38]. Moreover, the concomitant expression of VEGF ligands and VEGFR1 by tumor cells suggests that an autocrine VEGF/VEGFR1 signaling loop exists [37,38]. In addition, recently a novel angiogenesis-independent crosstalk between the VEGF and the EGF pathways was described in HCT116 colon cancer cells [38]. Interestingly, opposite to the effects we observed with our small molecule in A431 cells, inhibition of VEGFR-1 (by antibody treatment) resulted in downregulation of the EGFR signaling in HCT116 cells in this study. Thus, although our data support the hypothesis, that such a cross talk exists, there seem to be cell type- and drug-dependent differences.

Noteworthy, we found the synergism between KP2187 and sunitinib independent from the basal cellular VEGFR1 expression levels in several cell models. Thus, synergism was also seen in A431 cells, which were characterized by EGFR overexpression but basically undetectable VEGFR1 levels. VEGFR1 expression was also not induced by KP2187 or sunitinib (data not shown). In contrast, we observed that sunitinib resulted in further stimulation of EGFR phosphorylation in cell culture as well as *in vivo*. To the best of our knowledge, this has not been reported so far. Consequently, more in-depth follow up studies are needed not only to elucidate the underlying mechanisms of this phenomenon but also to evaluate whether it is A431-specific or a common phenomenon also in other cell lines.

Taken together, we showed that the chelating moiety of KP2187 is not interfering with its EGFR-inhibitory function. Therefore, KP2187 is a potent new EGFR inhibitor candidate for further prodrug development. Moreover, we showed that our inhibitor synergizes with VEGFR inhibition *in vitro* as well as *in vivo* independent from the cellular VEGFR1 status.

Consent for publication

All authors agree with the content of the paper and are listed as co-authors.

Funding details

This project was financed the Austrian Science Fund (FWF) projects FG3 to PH as well as P28853 to CRK.

CRediT authorship contribution statement

Monika Caban: Data curation, Formal analysis, Investigation, Methodology, Validation, Visualization, Writing – original draft, Writing – review & editing. **Bettina Koblmueller:** Conceptualization, Data curation, Investigation, Methodology, Validation, Visualization, Writing – original draft. **Diana Groza:** Conceptualization, Investigation. **Hemma H. Schueffl:** Data curation, Investigation, Methodology, Writing – review & editing. **Alessio Terenzi:** Formal analysis, Investigation, Methodology, Validation, Visualization, Writing – original draft. **Alexander Tolios:** Formal analysis, Investigation, Methodology, Validation, Writing – original draft. **Thomas Mohr:** Data curation, Writing – review & editing. **Marlene Mathuber:** Formal analysis, Investigation, Methodology, Visualization, Writing – review & editing. **Kushtrim Kryeziu:** Data curation, Investigation, Methodology. **Carola Jaunecker:** Data curation, Methodology. **Christine Pirker:** Data curation, Investigation, Methodology, Writing – review & editing. **Bernhard K. Keppler:** Supervision, Writing – review & editing. **Walter Berger:** Conceptualization, Supervision, Writing – review & editing. **Christian R. Kowol:** Conceptualization, Supervision, Visualization, Writing – original draft, Writing – review & editing. **Petra Heffeter:** Conceptualization, Data curation, Investigation, Methodology, Project administration, Resources, Supervision, Validation, Visualization, Writing – original draft, Writing – review & editing.

Declaration of competing interest

The authors declare that they have no known competing financial interests or personal relationships that could have appeared to influence the work reported in this paper.

Acknowledgements

We thank Gerhard Zeitler (Center for Cancer Research, Vienna) for devoted animal care and Gerald Timelthaler (Center for Cancer Research, Vienna) for help with the digital tissue analysis. Many thanks to Xenia Hudec (Center for Cancer Research) for technical assistance.

Appendix A. Supplementary data

Supplementary data to this article can be found online at https://doi.org/10.1016/j.canlet.2023.216237.

References

[1] V. Hofman, P. Hofman, Resistances to EGFR tyrosine kinase inhibitors in lung cancer-how to routinely track them in a molecular pathology laboratory? J. Thorac. Dis. 11 (2019) S65–S70.
[2] P. Kozakiewicz, L. Grzybowska-Szatkowska, Application of molecular targeted therapies in the treatment of head and neck squamous cell carcinoma (Review), Oncol. Lett. 15 (5) (2018) 7497–7505.
[3] D.E. Johnson, et al., Head and neck squamous cell carcinoma, Nat. Rev. Dis. Prim. 6 (1) (2020) 92.
[4] L.H. Biller, D. Schrag, Diagnosis and treatment of metastatic colorectal cancer: a review, JAMA 325 (7) (2021) 669–685.
[5] J. Yang, J. Yan, B. Liu, Targeting EGFRvIII for glioblastoma multiforme, Cancer Lett. 403 (2017) 224–230.
[6] A. Ayati, et al., A review on progression of epidermal growth factor receptor (EGFR) inhibitors as an efficient approach in cancer targeted therapy, Bioorg. Chem. 99 (2020), 103811.
[7] S. Wang, Y. Song, D. Liu, EAI045: the fourth-generation EGFR inhibitor overcoming T790M and C797S resistance, Cancer Lett. 385 (2017) 51–54.
[8] Z.H. Tang, J.J. Lu, Osimertinib resistance in non-small cell lung cancer: mechanisms and therapeutic strategies, Cancer Lett. 420 (2018) 242–246.
[9] B. Sharma, V.J. Singh, P.A. Chawla, Epidermal growth factor receptor inhibitors as potential anticancer agents: an update of recent progress, Bioorg. Chem. 116 (2021), 105393.
[10] R. Pérez-Soler, Can rash associated with HER1/EGFR inhibition be used as a marker of treatment outcome? Oncology 17 (11 Suppl 12) (2003) 23–28.
[11] Y. Kiyohara, N. Yamazaki, A. Kishi, Erlotinib-related skin toxicities: treatment strategies in patients with metastatic non-small cell lung cancer, J. Am. Acad. Dermatol. 69 (3) (2013) 463–472.
[12] B.C. Agema, et al., Improving the tolerability of osimertinib by identifying its toxic limit, Ther. Adv. Med. Oncol. 14 (2022), 17588359221103212.
[13] A. Ríos-Hoyo, L. Moliner, E. Arriola, Acquired mechanisms of resistance to osimertinib-the next challenge, Cancers 14 (8) (2022).
[14] M. Takeda, K. Nakagawa, First- and second-generation EGFR-TKIs are all replaced to osimertinib in chemo-naive EGFR mutation-positive non-small cell lung cancer? Int. J. Mol. Sci. 20 (1) (2019).
[15] X. Le, et al., Dual EGFR-VEGF pathway inhibition: a promising strategy for patients with EGFR-mutant NSCLC, J. Thorac. Oncol. 16 (2) (2021) 205–215.
[16] C.W.S. Tong, et al., Drug combination approach to overcome resistance to EGFR tyrosine kinase inhibitors in lung cancer, Cancer Lett. 405 (2017) 100–110.
[17] C. Karnthaler-Benbakka, et al., Tumor-targeting of EGFR inhibitors by hypoxia-mediated activation, Angew Chem. Int. Ed. Engl. 53 (47) (2014) 12930–12935.
[18] C. Karnthaler-Benbakka, et al., Targeting a targeted drug: an approach toward hypoxia-activatable tyrosine kinase inhibitor prodrugs, ChemMedChem 11 (21) (2016) 2410–2421.
[19] G.M. Morris, et al., AutoDock4 and AutoDockTools4: automated docking with selective receptor flexibility, J. Comput. Chem. 30 (16) (2009) 2785–2791.
[20] M.J. Frisch, et al., Gaussian 16 Rev. C.01, 2016 (Wallingford, CT).
[21] A.D. Becke, Density-functional thermochemistry .3. The role of exact exchange, J. Chem. Phys. 98 (7) (1993) 5648–5652.

[22] R.A. Laskowski, M.B. Swindells, LigPlot+: multiple ligand-protein interaction diagrams for drug discovery, J. Chem. Inf. Model. 51 (10) (2011) 2778–2786.
[23] E.F. Pettersen, et al., UCSF Chimera–a visualization system for exploratory research and analysis, J. Comput. Chem. 25 (13) (2004) 1605–1612.
[24] P. Heffeter, et al., Multidrug-resistant cancer cells are preferential targets of the new antineoplastic lanthanum compound KP772 (FFC24), Biochem. Pharmacol. 73 (12) (2007) 1873–1886.
[25] R.C.R. Team, A Language and Environment for Statistical Computing, R Foundation for Statistical Computing, Vienna, 2018. Available from: https://www.R-project.org.
[26] B.D. Ripley, Modern Applied Statistics with S, fourth ed., Springer, 2002.
[27] L. Meng, et al., A novel lead compound CM-118: antitumor activity and new insight into the molecular mechanism and combination therapy strategy in c-Met- and ALK-dependent cancers, Cancer Biol. Ther. 15 (6) (2014) 721–734.
[28] T. Friess, W. Scheuer, M. Hasmann, Erlotinib antitumor activity in non-small cell lung cancer models is independent of HER1 and HER2 overexpression, Anticancer Res. 26 (5a) (2006) 3505–3512.
[29] B.A. Helfrich, et al., Antitumor activity of the epidermal growth factor receptor (EGFR) tyrosine kinase inhibitor gefitinib (ZD1839, Iressa) in non-small cell lung cancer cell lines correlates with gene copy number and EGFR mutations but not EGFR protein levels, Clin. Cancer Res. 12 (23) (2006) 7117–7125.
[30] A. Mahipal, N. Kothari, S. Gupta, Epidermal growth factor receptor inhibitors: coming of age, Cancer Control 21 (1) (2014) 74–79.
[31] K. Suda, et al., Reciprocal and complementary role of MET amplification and EGFR T790M mutation in acquired resistance to kinase inhibitors in lung cancer, Clin. Cancer Res. 16 (22) (2010) 5489–5498.
[32] M.M. Attwood, et al., Trends in kinase drug discovery: targets, indications and inhibitor design, Nat. Rev. Drug Discov. 20 (11) (2021) 839–861.
[33] F.M. Ferguson, N.S. Gray, Kinase inhibitors: the road ahead, Nat. Rev. Drug Discov. 17 (5) (2018) 353–377.
[34] L. Huang, S. Jiang, Y. Shi, Tyrosine kinase inhibitors for solid tumors in the past 20 years (2001–2020), J. Hematol. Oncol. 13 (1) (2020) 143.
[35] K.S. Bhullar, et al., Kinase-targeted cancer therapies: progress, challenges and future directions, Mol. Cancer 17 (1) (2018) 48.
[36] G.V. Scagliotti, et al., Sunitinib plus erlotinib versus placebo plus erlotinib in patients with previously treated advanced non-small-cell lung cancer: a phase III trial, J. Clin. Oncol. 30 (17) (2012) 2070–2078.
[37] B.M. Lichtenberger, et al., Autocrine VEGF signaling synergizes with EGFR in tumor cells to promote epithelial cancer development, Cell 140 (2) (2010) 268–279.
[38] H. Nagano, et al., VEGFR-1 regulates EGF-R to promote proliferation in colon cancer cells, Int. J. Mol. Sci. 20 (22) (2019).